Magnetic structure of $Cu_2CdB_2O_6$ exhibiting a quantum-mechanical magnetization plateau and classical antiferromagnetic long-range order

Masashi Hase,[1,*] Andreas Dönni,[1] Vladimir Yu. Pomjakushin,[2] Lukas Keller,[2] Fabia Gozzo,[3] Antonio Cervellino,[3] and Masanori Kohno[1]

[1]*National Institute for Materials Science (NIMS), 1-2-1 Sengen, Tsukuba, Ibaraki 305-0047, Japan*

[2]*Laboratory for Neutron Scattering, ETH Zurich and Paul Scherrer Institut (PSI), CH-5232 Villigen, Switzerland*

[3]*Swiss Light Source, Paul Scherrer Institut (PSI), CH-5232 Villigen, Switzerland*

(Received 18 May 2009; revised manuscript received 12 August 2009; published 4 September 2009)

In $Cu_2CdB_2O_6$, a quantum-mechanical 1/2 magnetization plateau and classical antiferromagnetic long-range order (AF-LRO) appear. Two crystallographic Cu sites (Cu1 and Cu2) exist and have spin-1/2. It was speculated previously that spins on the Cu1 sites were in a nearly singlet state and that spins on the Cu2 sites formed the long-range order in weak magnetic fields and were almost saturated in fields of the magnetization plateau. As described herein, we report the magnetic structure of $Cu_2{}^{114}Cd^{11}B_2O_6$ as determined using neutron powder-diffraction measurements. Contrary to that previous speculation, both the Cu1 and Cu2 spins have large magnetic moments in the ordered state. We discuss the mechanism which causes the magnetization plateau and AF-LRO.

DOI: 10.1103/PhysRevB.80.104405 PACS number(s): 75.25.+z, 75.45.+j, 75.10.Jm, 75.50.Ee

I. INTRODUCTION

Magnetic long-range order (LRO) does not appear at finite temperature in low-dimensional antiferromagnetic (AF) Heisenberg spin systems. Supplementary interactions such as interchain interactions in one-dimensional spin systems (spin chains) sometimes stabilize magnetic LRO. Magnetic LROs in low-dimensional spin systems often differ from those in three-dimensional (3D) spin systems as cubic systems. An example is antiferromagnetic long-range order (AF-LRO) in the spin-chain cuprate $CuGeO_3$ doped with impurities.[1,2] This cuprate exhibits the spin-Peierls transition[3,4] instead of AF-LRO in spite of finite interchain interactions.[5] The AF-LRO induced by doping of impurities is accompanied by a spatial modulation of magnitude of magnetic moments and spin-gap excitations.[6–9]

The spin state at low temperature in the low-dimensional antiferromagnet $Cu_2CdB_2O_6$ was speculated to be peculiar.[10] This substance exhibits a quantum-mechanical 1/2 magnetization plateau as well as classical AF-LRO. Only Cu^{2+} ions have spin-1/2. Figure 1(a) schematically presents Cu positions[11] and dominant exchange interactions.[10] Two crystallographic Cu sites (Cu1 and Cu2) exist. Two Cu^{2+} ions in the Cu-Cu bond 1, 2, or 3 share one or two O^{2-} ions. The parameters of the exchange interaction are defined respectively as J_1, J_2, and J_3 for the Cu-Cu bonds 1, 2, and 3. A spin Hamiltonian formed by the three interactions is expressed as

$$\mathcal{H} = \sum_i [J_1 S_{i,2} \cdot S_{i,3} + J_2(S_{i,1} \cdot S_{i,2} + S_{i,3} \cdot S_{i,4}) + J_3(S_{i,1} \cdot S_{i+1,1} + S_{i,4} \cdot S_{i+1,4})]. \quad (1)$$

The J_1 interactions form dimers of Cu1 spins. The J_3 interactions form chains of Cu2 spins. The J_2 interactions connect dimers and chains.

In the previous work,[10] we assumed that the three interactions were AF because Cu-O-Cu angles are larger than 99° in the three bonds. We calculated the temperature T dependence of the magnetic susceptibility $\chi(T)$ and the magnetic-field H dependence of the magnetization $M(H)$ of the spin system shown in Fig. 1(a) and described by Hamiltonian (1). We obtained calculated results which well fitted the experimental ones in the whole temperature range. Obtained values of the three interactions seemed reasonable. Therefore, we considered that we needed not include explicitly other interactions in the model to explain the magnetism of $Cu_2CdB_2O_6$. However, the three interactions alone leave the spin system fractured into groups of dimers and two chains. Therefore, AF-LRO cannot be generated only by the J_1, J_2, and J_3 interactions. Other weak 3D interactions and anisotropy are necessary to stabilize AF-LRO.

In the previous work,[10] the J1 interaction was evaluated to be the strongest. It was speculated that a state of Cu1 spins was nearly nonmagnetic with an energy gap because of an AF dimer formed by the strongest J_1 interaction and that Cu2 spins formed AF-LRO in low magnetic fields and were almost saturated at fields stronger than 23 T. This picture can explain a 1/2 magnetization plateau.

In the present work, we report the magnetic structure below the AF transition temperature $T_N = 9.8$ K in $Cu_2CdB_2O_6$ determined using neutron powder-diffraction measurements. Contrary to the previous speculation,[10] the Cu1 spins as well as the Cu2 spins are found to have large magnetic moments as low-dimensional antiferromagnets. We discuss the reason why the quantum-mechanical 1/2 magnetization plateau and classical AF-LRO can appear.

II. METHODS OF EXPERIMENTS AND CALCULATIONS

Crystalline powders of $Cu_2{}^{114}Cd^{11}B_2O_6$ were synthesized using a solid-state-reaction method at 1073 K in air for 160 h with intermediate grindings. We used isotopes ^{114}Cd and ^{11}B to decrease the absorption of neutrons. Purity of the isotopes is 99%. We confirmed formation of $Cu_2CdB_2O_6$ using an x-ray diffractometer (JDX-3500; JEOL).

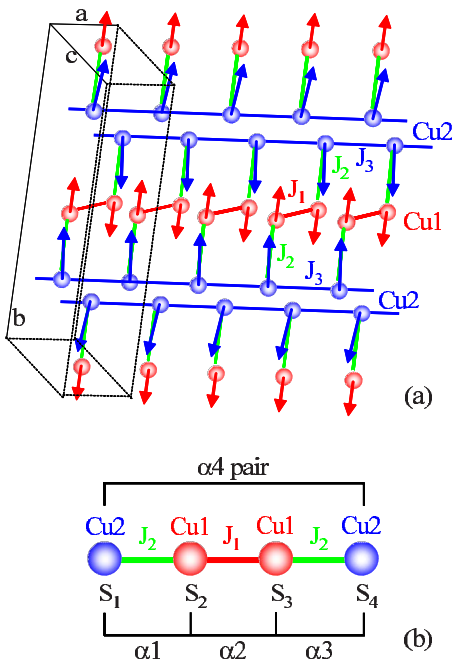

FIG. 1. (Color online) (a) A schematic drawing of Cu^{2+}-ion positions in $Cu_2CdB_2O_6$. Red and blue circles represent Cu1 and Cu2 sites, respectively. Red, green, and blue bars represent Cu-Cu bonds 1, 2, and 3, respectively. Parameters of an exchange interaction are defined, respectively, as J_1, J_2, and J_3 in the Cu-Cu bond 1, 2, and 3. Arrows on the Cu sites indicate magnetic moments below T_N=9.8 K determined in the present study. A box on the left side shows the crystallographic unit cell. (b) An illustration of the four-spin system consisting of S_1–S_4. We designate a spin pair formed by S_j and S_{j+1} as an α_j pair.

We have investigated temperature dependence of lattice parameters in detail by means of high-resolution synchrotron radiation x-ray powder-diffraction experiments. The experiments were performed using the high-resolution Materials Science powder diffractometer (MS-PD) (wavelength λ =0.4974 Å) at the Swiss Light Source Materials Science (SLS-MS) beamline at the Paul Scherrer Institut (PSI) in Switzerland. Powders were loaded in a 0.3-mm-diameter and 30-mm-long Lindemann capillary to reduce the effect of the absorption. The capillary spun at approximately 6 Hz for improved powder averaging inside the ^{4}He cryostat (Janis, T range; 4.2–300 K). The diffracted signal was detected using the high-resolution fast MYTHEN II solid-state detector.[12] Thanks to the extremely high counting efficiency of MYTHEN II we were able to follow the T evolution of the lattice parameters at very fine steps (approximately 1 K step below 11 K; approximately 2 K step from 13 to 20 K; approximately 5 K step from 25 to 300 K).

We determined the magnetic structure of $Cu_2{}^{114}Cd{}^{11}B_2O_6$ from neutron powder-diffraction experiments. The experiments were conducted using the high-resolution powder diffractometer for thermal neutrons (HRPT) (λ=1.886 Å) and the high-intensity cold neutron powder diffractometer (DMC) (λ=2.458 Å) at the Swiss spallation neutron source SINQ at PSI. Powders were packed in a vanadium container with 8 mm diameter and 55 mm height. The container was installed in an orange cryostat. The temperature range was

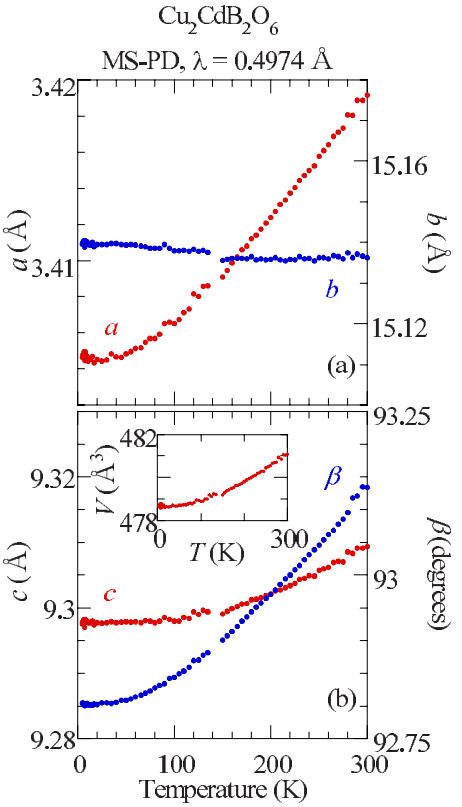

FIG. 2. (Color online) Temperature dependence of lattice parameters in $Cu_2{}^{114}Cd{}^{11}B_2O_6$ determined using the synchrotron x-ray diffractometer MS-PD (λ=0.4974 Å).

1.5–15 K. Rietveld refinements of diffraction data were performed using the FULLPROF program package.[13] Symmetry analyses of possible magnetic configurations were conducted using the program BASIREP in the FULLPROF program package.

We calculated susceptibility and magnetization of the spin system shown in Fig. 1(a) and described by Hamiltonian (1) using a quantum Monte Carlo (QMC) technique with a directed-loop algorithm in path-integral formulation.[14] The respective quantities of sites and Monte Carlo samples in QMC simulations are one thousand and about one million. Finite-size effects and statistical errors are negligible in the scales of figures represented in this paper.

III. RESULTS AND DISCUSSION

The space group of $Cu_2CdB_2O_6$ is monoclinic $P2_1/c$ (No. 14).[11] Figure 2 portrays the temperature dependence of lattice parameters determined using the synchrotron x-ray diffractometer MS-PD. Values of $(y_{max}-y_{min})/(y_{max}+y_{min})$ are set to about 0.0026 in the main figures to facilitate comparison of the relative changes of these parameters. Here, y_{max} and y_{min}, respectively, denote values of upper and lower limits of each vertical axis. As the temperature is lowered, a, c, and β decrease, whereas b slightly increases. The volume of the unit cell decreases concomitantly with decreasing T. The ratio between maximum and minimum values of a is 1.004. Therefore, the temperature dependence of lattice parameters

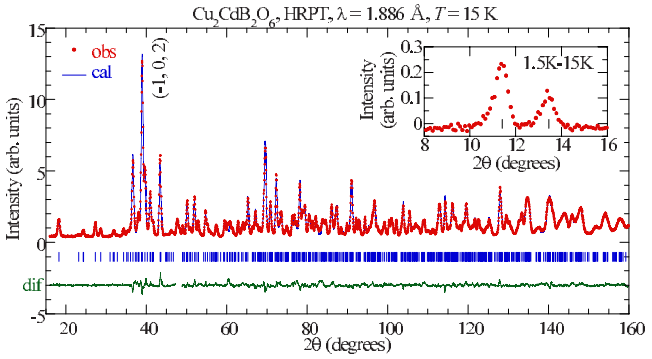

FIG. 3. (Color online) A neutron powder-diffraction pattern of $Cu_2{}^{114}Cd^{11}B_2O_6$ at 15 K (higher than T_N) measured using the HRPT diffractometer ($\lambda=1.886$ Å). Lines on the observed pattern and at the bottom show a Rietveld refined pattern and difference between the observed and the Rietveld refined patterns. The observed data between 47.2° and 48.8° were not used in the refinement because a weak reflection of an impurity phase exists. Short vertical lines represent positions of nuclear reflections. The strongest nuclear reflection (−1, 0, 2) is indexed. The inset depicts differences between the HRPT patterns measured at 1.5 and 15 K. Two strong magnetic reflections indexed by (0,0,1) and (0,1,1) are, respectively, apparent at 11.4° and 13.4°.

is small. Probably, the values of exchange interactions are almost independent of T. The lattice parameters do not show remarkable changes around $T_N=9.8$ K. Magnetism does not couple with the lattice system.

Figure 3 depicts the neutron powder-diffraction pattern of paramagnetic $Cu_2{}^{114}Cd^{11}B_2O_6$ recorded using the HRPT diffractometer with $\lambda=1.886$ Å at 15 K, which is slightly higher than $T_N=9.8$ K. We determined the crystal structure using a FULLPROF refinement based on 753 inequivalent nuclear reflections within the monoclinic space group $P2_1/c$ and all atoms on the most general site 4*e*. The FULLPROF refinement based on the crystal structure of $Cu_2CdB_2O_6$ as determined by room-temperature single-crystal x-ray diffraction[11] can well reproduce the observed neutron-diffraction data at 15 K. Structural parameters are presented in Table I; interatomic distances and angles of the three Cu-Cu bonds at 15 K presented in Table II.

The inset of Fig. 3 depicts the difference between two neutron powder-diffraction patterns recorded at 1.5 and 15 K. Additional weak reflections are apparent at 1.5 K. As explained later, these are magnetic reflections caused by the AF-LRO. The magnetic reflections at 11.4° and 13.4° can be indexed respectively as (0,0,1) and (0,1,1) and have the strongest intensities among all magnetic reflections. Nevertheless, these intensities are two orders of magnitude less than the intensity of the strongest nuclear reflection (−1,0,2) at 39.0°.

Dots presented in Fig. 4 represent the difference between two neutron powder-diffraction patterns recorded at 1.5 and 15 K using the DMC diffractometer with $\lambda=2.458$ Å. The new reflections at 1.5 K can all be indexed with a propagation vector $\mathbf{k}=[0,0,0]$. Some new reflections exist on positions of nuclear reflections, whereas indices of the others are $(0,k,0)$ with odd k, $(0,0,l)$ with odd l, or $(h,0,l)$ with odd h and l. The inset of Fig. 4 portrays the temperature dependence of integrated intensity of the magnetic reflection at (0,0,1). This reflection appears below $T_N=9.8$ K. The intensity increases with decreasing T and is saturated at less than 4 K. The temperature dependence indicates that the new reflections in Fig. 4 are magnetic reflections.

TABLE I. Structural parameters of $Cu_2CdB_2O_6$ derived from Rietveld refinement of the HRPT neutron powder-diffraction pattern at 15 K. The space group is monoclinic $P2_1/c$ (No. 14). The lattice constants at 15 K based on the more accurate x-ray diffraction data are $a=3.4047(5)$ Å, $b=15.140(2)$ Å, $c=9.298(1)$ Å, and $\beta=92.80(1)°$. To reduce the large number of fitting parameters, one Debye-Waller factor was used for each element. Estimated standard deviations are shown in parentheses. Agreement values of the fit were $R_{wp}=6.94\%$, $R_{\text{expt.}}=2.69\%$, and $\chi^2=6.66$.

Atom	Site	x	y	z	B_{iso} (Å^2)
Cu1	4*e*	0.3116(9)	0.5396(2)	0.3687(3)	0.43(4)
Cu2	4*e*	0.3083(9)	0.7473(2)	0.8699(3)	0.43(4)
Cd1	4*e*	0.2031(13)	0.3685(3)	0.8836(5)	0.72(12)
B1	4*e*	0.1994(10)	0.3458(3)	0.4197(3)	0.73(6)
B2	4*e*	0.8744(12)	0.4114(3)	0.1866(4)	0.73(6)
O1	4*e*	0.2439(13)	0.2709(2)	0.4924(5)	0.68(4)
O2	4*e*	0.3153(12)	0.8523(3)	0.7634(4)	0.68(4)
O3	4*e*	0.3334(12)	0.4268(3)	0.4689(5)	0.68(4)
O4	4*e*	0.7123(11)	0.3772(3)	0.0624(4)	0.68(4)
O5	4*e*	0.0670(12)	0.5031(3)	0.7779(5)	0.68(4)
O6	4*e*	0.0058(11)	0.3424(3)	0.2802(4)	0.68(4)

Using the magnetic propagation vector $\mathbf{k}=[0,0,0]$, we performed a symmetry analysis according to Izyumov *et al.*[15] to derive possible magnetic configurations for both Cu(4*e*) sites of the space group $P2_1/c$. The symmetry analysis allows four irreducible representations (IRs), as shown in Table III. The observed magnetic patterns were compared with calculated patterns using the structural parameters of both Cu1 and Cu2 determined from the structural refinement. After sorting out the basis functions of all four IRs, we found that only τ_2 well fits the observed pattern. The intensities of the weak magnetic reflections at 2θ values around 40°–50° are essential to select the correct IR.

The magnetic structure is depicted in Fig. 1(a). The magnetic moment vector at the Cu1(1) position is $[0.05(5), -0.44(2), -0.04(4)]\mu_B$, and its magnitude is $0.45(2)\mu_B$ for a g value of 2. The ordered Cu1 moments almost point along the b direction and components along a and c directions are zero within experimental errors. The magnetic moment vector at the Cu2(1) position is $[-0.16(7), 0.81(2), 0.1(2)]\mu_B$, and its magnitude is $0.83(3)\mu_B$ for a g value of 2. The ordered Cu2 moments almost point along the b direction with a small component along the a direction. The three-dimensional arrangement of the moments indicates that the J_1, J_2, and J_3 interactions are AF, ferromagnetic (F), and F, respectively. The signs of the J_2 and J_3 interactions are opposite to those obtained in the previous paper. In the previous paper,[10] it was speculated that the Cu1 moment was very small and that only the Cu2 moment was effective and

TABLE II. Interatomic distances and angles at 15 K in $Cu_2CdB_2O_6$.

	Cu-Cu distance (Å)	Cu-O-Cu path	Angle (deg)	Cu-O distance (Å)	Number of path
Bond 1 (J_1)	2.96 Cu1-Cu1	Cu1-O3-Cu1	98.4	1.94, 1.95	2
Bond 2 (J_2)	3.23 Cu1-Cu2	Cu1-O2-Cu2	117	1.91, 1.87	1
Bond 3 (J_3)	3.41 Cu2-Cu2	Cu2-O1-Cu2	103	1.97, 2.35	1

formed AF-LRO. Contrary to that speculation, both the Cu1 and Cu2 spins have large magnetic moments as low-dimensional antiferromagnets.

We now determine values of the exchange interactions. We can estimate as $j \equiv J_2/J_1 = -0.54(6)$ from a ratio of the values of the two magnetic moments $(0.45/0.83 = 0.54)$.[16] Experimental susceptibility is roughly reproduced by calculated susceptibility with $J_1 = 240$ K, $J_2 = jJ_1 = -130$ K, and $J_3 = 0$ K (not shown). We consider the J_3 interaction. QMC results with $J_1 = 264$ K, $J_2 = jJ_1 = -143$ K, and $J_3 = -4.95$ K well fit the experimental susceptibility above $T_N = 9.8$ K and magnetization at 15 K (above T_N), as presented in Figs. 5(a) and 5(b), respectively. A 1/2 magnetization plateau appears at around 20 T in an experimental magnetization curve and QMC results of magnetization at 2.9 K, as presented in Fig. 5(c). The experimental curve in low magnetic fields, however, cannot be reproduced by the QMC results of magnetization. We calculated susceptibility and magnetization using several values of the three interactions for the case $j < 0$. However, within the case $j < 0$ we were unable to find values of the exchange interactions which can reproduce experimental results at all temperatures. The discrepancy between the experimental and QMC results below T_N is probably caused by the formation of AF-LRO which cannot be explained by the spin system shown in Fig. 1(a) and described by Hamiltonian (1). As presented in Table II, one of the Cu2-O1 distances in the bond 3 is large (2.35 Å). Accordingly, we consider that the magnitude of the J_3 value is much smaller than that of the J_1 and J_2 values.

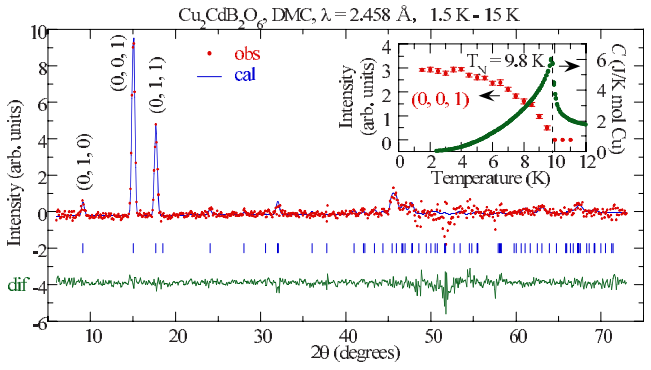

FIG. 4. (Color online) Difference between two neutron powder-diffraction patterns of $Cu_2{}^{114}Cd^{11}B_2O_6$ at 1.5 and 15 K recorded using the DMC diffractometer ($\lambda = 2.458$ Å). Lines on the observed pattern and at the bottom show a Rietveld refined pattern and difference between the observed and the Rietveld refined patterns. Short vertical lines represent positions of magnetic reflections. The strong magnetic reflections (0,1,0), (0,0,1), and (0,1,1) are indexed. The inset shows the temperature dependence of integrated intensity of the magnetic reflection at (0,0,1). The inset also depicts specific heat to indicate the AF transition temperature (T_N) (Ref. 10).

We discuss why the quantum-mechanical 1/2 magnetization plateau and the classical AF-LRO can appear in $Cu_2CdB_2O_6$. Classical models of AF-LRO cannot explain the 1/2 magnetization plateau. As described, all the magnetic moment vectors are almost parallel to the b direction. When magnetic fields are applied perpendicular to the b direction, magnetization increases gradually up to a saturation field. When magnetic fields are applied parallel to the b direction, magnetization also increases up to a saturation field. A rapid increase in magnetization is apparent at the spin-flop transition. Magnetization plateaus cannot appear when the magnetization in AF-LRO is considered based on classical models. Accordingly, the 1/2 magnetization plateau in $Cu_2CdB_2O_6$ is caused by quantum-mechanical discrete energy levels of magnetic eigenstates.

We consider eigenstates of the spin system in $Cu_2CdB_2O_6$. The J_1 and J_2 interactions are dominant. Therefore, it is expected that the eigenstates in $Cu_2CdB_2O_6$ resemble those of the four-spin system depicted in Fig. 1(b). Eigenenergies and eigenstates of the four-spin system have already been calculated.[17] There are two $S^T = 0$ states ($|01\rangle$ and $|02\rangle$), three $S^T = 1$ states ($|11\rangle$, $|12\rangle$, and $|13\rangle$), and one $S^T = 2$ state ($|21\rangle$). S^T means a total spin of the four-spin system. When $J_1 = 264$ K and $J_2 = -143$ K, the ground state (GS) in the zero magnetic field is $|02\rangle$. Energy difference between GS and excited states is 16.6 ($|13\rangle$), 227 ($|21\rangle$), 317 ($|12\rangle$), 370 ($|11\rangle$), and 477 K ($|01\rangle$). As the magnetic field

TABLE III. Characters of irreducible representations (IRs) of a little group of the propagation vector $\mathbf{k} = [0,0,0]$ for the space group $P2_1/c$. The basis vectors of IR (τ_2) ψ_1, ψ_2, and ψ_3 are also given. Decompositions of axial vector representations for the 4e site read as $\Gamma_{Mag} = 3\tau_1 \oplus 3\tau_2 \oplus 3\tau_3 \oplus 3\tau_4$.

IR/symmetry operation	(1) x,y,z	(2) $\bar{x},y+\frac{1}{2},\bar{z}+\frac{1}{2}$	(3) $\bar{x},\bar{y},\bar{z}$	(4) $x,\bar{y}+\frac{1}{2},z+\frac{1}{2}$
		Characters of IR		
τ_1	1	1	1	1
τ_2	1	1	−1	−1
τ_3	1	−1	1	−1
τ_4	1	−1	−1	1
		Basis vectors of IR (τ_2)		
ψ_1	(100)	$(\bar{1}00)$	$(\bar{1}00)$	(100)
ψ_2	(010)	(010)	$(0\bar{1}0)$	$(0\bar{1}0)$
ψ_3	(001)	$(00\bar{1})$	$(00\bar{1})$	(001)

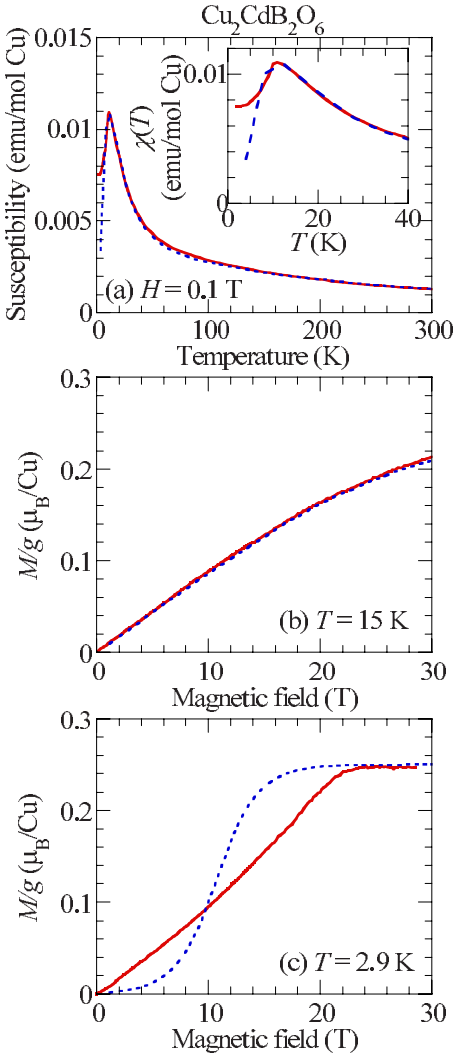

FIG. 5. (Color online) (a) The temperature dependence of the experimental susceptibility (red solid curve) and QMC results of susceptibility (blue dashed curve) less than 300 K. The inset shows the susceptibility less than 40 K. (b) The magnetic field dependence of experimental magnetization (red solid curve) and QMC results of magnetization (blue dashed curve) at 15 K. (c) The magnetic field dependence of experimental magnetization (red solid curve) and QMC results of magnetization (blue dashed curve) at 2.9 K.

increases, GS moves sequentially to $|13,S_z^{\mathrm{T}}=1\rangle$ and to $|21,S_z^{\mathrm{T}}=2\rangle$. The magnetization of the four-spin system exhibits a 1/2 magnetization plateau because of the energy difference between $|13\rangle$ and $|21\rangle$. The ground state in magnetic fields of the magnetization plateau (plateau region) is expressed as

$$|13,S_z^{\mathrm{T}}=1\rangle = C_{11}(|+-++\rangle - |++-+\rangle) + C_{12}(|-+++\rangle - |+++-\rangle)$$

$$= C_{11}(|-+\rangle - |+-\rangle)_{\alpha 2} * |++\rangle_{\alpha 4} + C_{12}(|-+\rangle - |+-\rangle)_{\alpha 4} * |++\rangle_{\alpha 2}. \quad (2)$$

The two coefficients are

$$C_{11} = \frac{1+j+\sqrt{1+j^2}}{2\sqrt{1+(j+\sqrt{1+j^2})^2}}, \quad (3)$$

$$C_{12} = \frac{1-j-\sqrt{1+j^2}}{2\sqrt{1+(j+\sqrt{1+j^2})^2}}. \quad (4)$$

The sign + or − in kets $|\ldots.\rangle$ means $S_{jz}=1/2$ or $-1/2$ ($j=1$ to 4). For example, $|+-++\rangle$ means $|S_{1z}=1/2,S_{2z}=-1/2,S_{3z}=1/2,S_{4z}=1/2\rangle$. The first term in Eq. (2) is a product of a singlet state in the α_2 pair and a triplet state with $S_z=1$ in the α_4 pair. The second term in Eq. (2) is a product of a singlet state in the α_4 pair and a triplet state with $S_z=1$ in the α_2 pair. When $j=-0.54$, $C_{11}/C_{12}=3.9$. These results demonstrate that the Cu1 and Cu2 spins can simultaneously have characters of both singlet and triplet states.

In the four-spin system with $J_1=264$ K and $J_2=-143$ K, the energy difference between the singlet GS $|02\rangle$ and the first excited triplet state $|13\rangle$ is small in the zero magnetic field (16.6 K). Probably characters of the triplet states can be easily mixed into the singlet GS by introduction of other interactions except for the J_1 and J_2 interactions. Therefore, finite magnetic moments can exist in GS of $Cu_2CdB_2O_6$. AF-LRO, which differs greatly from the singlet state, is stabilized by the J_1, J_2, J_3, and other weak 3D interactions and anisotropy. There is no qualitative difference between Cu1 and Cu2 spins in the plateau region of the four-spin system.[18] Accordingly, it is expected that both the Cu1 and Cu2 spins have magnetic moments in the ordered state of $Cu_2CdB_2O_6$. The energy difference between the triplet state $|13\rangle$ and the $S^{\mathrm{T}}=2$ state $|21\rangle$ is large in the zero magnetic field (211 K). Characters of the $S^{\mathrm{T}}=2$ states cannot be easily mixed into the GS in the plateau region $|13,S_z^{\mathrm{T}}=1\rangle$. Therefore, the 1/2 magnetization plateau can remain. A magnetization plateau and magnetic LRO have been reported in several substances such as $A_3Cu_3(PO_4)_4$ (A=Ca,Sr,Pb),[19–21] $Cu_3(CO_3)_2(OH)_2$,[22] $(CH_3)_2NH_2CuCl_3$(DMACuCl$_3$),[23] and $AMn_3P_4O_{14}$ (A=Sr, Ba).[24] Their magnetic structures have not been investigated except for the observation of weak magnetic reflections in $Sr_3Cu_3(PO_4)_4$.[20] It is interesting to determine the magnetic structure of these substances and to study the relation between the magnetization plateau and magnetic LRO.

Let us now discuss anisotropy. Directions of ordered magnetic moments are determined mainly by anisotropy. Probably, oxygen positions around copper play an important role. We surveyed the relation between directions of ordered magnetic moments and oxygen positions around copper in several cuprates. Four short Cu-O bonds lie in a plane in La_2CuO_4 and $CuGeO_3$. Spins exist in $d(x^2-y^2)$ orbits spreading over the four Cu-O bonds. The ordered magnetic moments lie in the same plane.[6,25] The directions of the ordered moments avoid the four Cu-O bonds. In several cuprates where the four short Cu-O bonds do not lie in a plane, directions of ordered magnetic moments also seem to avoid the Cu-O bonds. Examples are $BaCu_2Ge_2O_7$ (Ref. 26) and $Cu_6Si_6O_{18}$-6H_2O.[27] A similar preference is also seen in $Cu_2CdB_2O_6$ as shown in Fig. 6.

At high temperatures, anisotropy energy is small enough compared to the temperature. Probably, we can evaluate val-

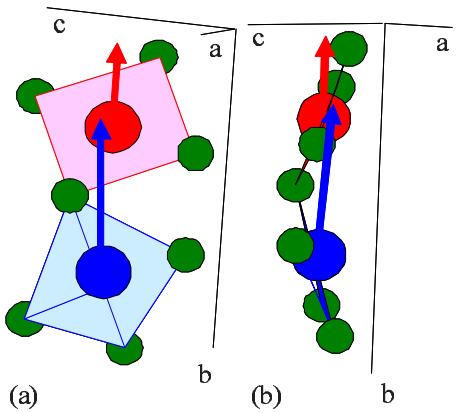

FIG. 6. (Color online) Schematic drawings portraying the relation between the directions of the ordered magnetic moments (arrows) and oxygen positions in $Cu_2CdB_2O_6$. The red large circles with the short arrow, blue large circles with the long arrow, and green small circles represent Cu1, Cu2, and O sites, respectively.

ues of dominant exchange interactions without considering anisotropy. As depicted in Fig. 5, we can quantitatively explain susceptibility and magnetization at temperatures greater than T_N using the spin system including the J_1, J_2, and J_3 interactions alone. Susceptibility and magnetization in the ordered state, on the other hand, cannot be reproduced by the same system. We have to add other energies. The next important energies are other weak 3D interactions which stabilize AF-LRO. In addition to the above-mentioned exchange interactions, anisotropy affects susceptibility and magnetization at low temperatures. However, it is impossible to determine uniquely values of these parameters because of the huge parameter space. We do not have formula of T_N and the spin-flop field H_{SF} of models including the J_1, J_2, J_3, and other weak 3D interactions and anisotropy. Therefore, we could not estimate these values from T_N or H_{SF}. As described in our previous paper,[10] H_{SF}=1.5 T=2.1 K. This value is much smaller than the J_1 or J_2 value (264 or −143 K). In a molecular field approximation for a two-sublattice model with one exchange interaction, H_{SF} is expressed as $H_{SF} = \sqrt{2H_E H_A}$. Here H_E or H_A is the magnetic field generated by the exchange interaction or anisotropy energy. Consequently, we can say that anisotropy is very small.

IV. CONCLUSIONS

$Cu_2CdB_2O_6$ exhibits the quantum-mechanical 1/2 magnetization plateau and classical antiferromagnetic long-range order. We determined the crystal and magnetic structure at low temperature using neutron and synchrotron x-ray powder-diffraction experiments. Contrary to the earlier speculation, the spins on both the Cu1 and Cu2 sites have large ordered magnetic moments as low-dimensional antiferromagnets. The 1/2 magnetization plateau is caused by the quantum-mechanical discrete energy levels of magnetic eigenstates of the four-spin system. The magnetization plateau remains against other weak three-dimensional interactions because of the large energy difference between the triplet and $S^T=2$ states. On the other hand, characters of the triplet state can be easily mixed into the singlet GS by introduction of the weak interactions because of the small energy difference between the singlet and triplet states. Therefore, finite magnetic moments can exist in GS of $Cu_2CdB_2O_6$. AF-LRO, which differs greatly from the singlet state, is stabilized by the J_1, J_2, J_3, and other weak 3D interactions and anisotropy. There is no qualitative difference between Cu1 and Cu2 spins in the plateau region of the four-spin system. Accordingly, it is expected that both the Cu1 and Cu2 spins have magnetic moments in the ordered state.

ACKNOWLEDGMENTS

We are grateful to M. Lange and D. Meister for the MS-PD experiments and to M. Kaise for the laboratory x-ray diffraction measurements. The neutron and synchrotron x-ray experiments were conducted at SINQ and SLS, PSI Villigen, Switzerland. This work was partially supported by grants from NIMS and by a Grant-in-Aid for Scientific Research from the Ministry of Education, Culture, Sports, Science, and Technology (MEXT).

*hase.masashi@nims.go.jp

[1] M. Hase, I. Terasaki, Y. Sasago, K. Uchinokura, and H. Obara, Phys. Rev. Lett. **71**, 4059 (1993).
[2] M. Hase, N. Koide, K. Manabe, Y. Sasago, K. Uchinokura, and A. Sawa, Physica B **215**, 164 (1995).
[3] M. Hase, I. Terasaki, and K. Uchinokura, Phys. Rev. Lett. **70**, 3651 (1993).
[4] M. Hase, I. Terasaki, K. Uchinokura, M. Tokunaga, N. Miura, and H. Obara, Phys. Rev. B **48**, 9616 (1993).
[5] M. Nishi, O. Fujita, and J. Akimitsu, Phys. Rev. B **50**, 6508 (1994).
[6] M. Hase, K. Uchinokura, R. J. Birgeneau, K. Hirota, and G. Shirane, J. Phys. Soc. Jpn. **65**, 1392 (1996).
[7] M. Hase, M. Hagiwara, and K. Katsumata, Phys. Rev. B **54**, R3722 (1996).
[8] M. C. Martin, M. Hase, K. Hirota, G. Shirane, Y. Sasago, N. Koide, and K. Uchinokura, Phys. Rev. B **56**, 3173 (1997).
[9] K. M. Kojima, Y. Fudamoto, M. Larkin, G. M. Luke, J. Merrin, B. Nachumi, Y. J. Uemura, M. Hase, Y. Sasago, K. Uchinokura, Y. Ajiro, A. Revcolevschi, and J.-P. Renard, Phys. Rev. Lett. **79**, 503 (1997).
[10] M. Hase, M. Kohno, H. Kitazawa, O. Suzuki, K. Ozawa, G. Kido, M. Imai, and X. Hu, Phys. Rev. B **72**, 172412 (2005).
[11] S. Münchau and K. Bluhm, Z. Naturforsch., B: Chem. Sci. **50**, 1151 (1995).
[12] B. Schmitt, C. Bronnimann, E. F. Eikenberry, G. Hulsen, H. Toyokawa, R. Horisberger, F. Gozzo, B. Patterson, C. Schulze-Briese, and T. Tomizaki, Nucl. Instrum. Methods Phys. Res. A **518**, 436 (2004).
[13] J. Rodriguez-Carvajal, Physica B **192**, 55 (1993).

[14] O. F. Syljuåsen and A. W. Sandvik, Phys. Rev. E **66**, 046701 (2002).
[15] Y. A. Izyumov, V. E. Naish, and R. P. Ozerov, *Neutron Diffraction of Magnetic Materials* (Consultants Bureau, New York, 1991).
[16] T. Masuda, A. Zheludev, B. Grenier, S. Imai, K. Uchinokura, E. Ressouche, and S. Park, Phys. Rev. Lett. **93**, 077202 (2004).
[17] M. Hase, K. M. S. Etheredge, S.-J. Hwu, K. Hirota, and G. Shirane, Phys. Rev. B **56**, 3231 (1997). In this reference, the spin Hamiltonian is defined as $\mathcal{H}=\Sigma 2J_h S_k \cdot S_l$ instead of $\mathcal{H}=\Sigma J_h S_k \cdot S_l$ in the present paper.
[18] When $J_1=264$ K and $J_2=-143$ K, a ground state in the zero magnetic field is one of the $S^T=0$ states and is expressed as $|02,S_z^T=0\rangle=C_{01}(|--++\rangle+|++--\rangle-|-+-+\rangle-|+-+-\rangle)+C_{02}(|-+-+\rangle+|+-+-\rangle-|+--+\rangle-|-++-\rangle)=C_{01}(|-+\rangle-|+-\rangle)_{\alpha 2}(|-+\rangle-|+-\rangle)_{\alpha 4}+C_{02}(|-+\rangle-|+-\rangle)_{\alpha 1}(|-+\rangle-|+-\rangle)_{\alpha 3}$. The two coefficients are $C_{01}=1/\sqrt{3+(-1+4j+2\sqrt{1-2j+4j^2})^2}$ and $C_{02}=(2-4j-2\sqrt{1-2j+4j^2})/2\sqrt{3+(-1+4j+2\sqrt{1-2j+4j^2})^2}$. The first term in $|02,S_z^T=0\rangle$ is a product of a singlet state in the α_2 pair and a singlet state in the α_4 pair. The second term is a product of a singlet state in the α_1 pair and a singlet state in the α_3 pair. The ground state is singlet. Therefore, we cannot determine whether Cu1 spins [S_2 and S_3 in Fig. 1(b)] and Cu2 spins [S_1 and S_4 in Fig. 1(b)] have magnetic moments or not.
[19] M. Drillon, M. Belaiche, P. Legoll, J. Aride, A. Boukhari, and A. Moqine, J. Magn. Magn. Mater. **128**, 83 (1993).
[20] Y. Ajiro, T. Asano, K. Nakaya, M. Mekata, K. Ohoyama, Y. Yamaguchi, Y. Koike, Y. Morii, K. Kamishima, H. Aruga-Katori, and T. Goto, in Proceedings of the International Symposium on Advances in Neutron Scattering Research, Tokai, 2000 [J. Phys. Soc. Jpn. 70, 186 (2001)].
[21] A. A. Belik, A. Matsuo, M. Azuma, K. Kindo, and M. Takano, J. Solid State Chem. **178**, 709 (2005).
[22] H. Kikuchi, Y. Fujii, M. Chiba, S. Mitsudo, T. Idehara, T. Tonegawa, K. Okamoto, T. Sakai, T. Kuwai, and H. Ohta, Phys. Rev. Lett. **94**, 227201 (2005).
[23] Y. Inagaki, A. Kobayashi, T. Asano, T. Sakon, H. Kitagawa, M. Motokawa, and Y. Ajiro, J. Phys. Soc. Jpn. **74**, 2683 (2005).
[24] T. Yang, Y. Zhang, S. Yang, G. Li, M. Xiong, F. Liao, and J. Lin, Inorg. Chem. **47**, 2562 (2008).
[25] D. Vaknin, S. K. Sinha, D. E. Moncton, D. C. Johnston, J. M. Newsam, C. R. Safinya, and H. E. King, Phys. Rev. Lett. **58**, 2802 (1987).
[26] I. Tsukada, J. Takeya, T. Masuda, and K. Uchinokura, Phys. Rev. B **62**, R6061 (2000).
[27] E. L. Belokoneva, Y. K. Gubina, J. B. Forsyth, and P. J. Brown, Phys. Chem. Miner. **29**, 430 (2002).